Available online at www.sciencedirect.com
ScienceDirect
Journal of Catalysis 254 (2008) 121–130
JOURNAL OF CATALYSIS
www.elsevier.com/locate/jcat

Palladium nanoparticles supported on alumina-based oxides as heterogeneous catalysts of the Suzuki–Miyaura reaction

Andrzej Gniewek [a], Józef J. Ziółkowski [a], Anna M. Trzeciak [a,*], Mirosław Zawadzki [b], Hanna Grabowska [b], Józef Wrzyszcz [b]

[a] *Faculty of Chemistry, University of Wrocław, 14 F. Joliot-Curie, 50-383 Wrocław, Poland*
[b] *Institute of Low Temperature and Structure Research, Polish Academy of Sciences, P.O. Box 1410, 50-950 Wrocław, Poland*

Received 5 November 2007; revised 12 December 2007; accepted 13 December 2007

Abstract

Alumina-based oxides Al_2O_3, Al_2O_3–ZrO_2 (A, B, C) and Al_2O_3–ZrO_2–Eu_2O_3 (D) were prepared by alkoxide sol–gel method and used as supports for palladium nanoparticles obtained by reduction of $PdCl_2$ by methanol or hydrazine. As confirmed by XRD and TEM methods, such catalysts are composed of palladium nanoparticles well dispersed on the surface of the alumina matrix. The Suzuki coupling of 2-bromotoluene with phenylboronic acid, used as the test reaction, revealed that the obtained catalysts were quite efficient even at 40 °C and that their catalytic activity increased at 60 and 80 °C. Very good results (95% yield after 1 h) also were obtained when $PdCl_2$ supported on mixed oxides was used without earlier palladium reduction. It was confirmed that under the reaction conditions, Pd(0) nanoparticles of ca. 5 nm in diameter were formed on the support. Under the same conditions (^{i}PrOH + H_2O used as a solvent, KOH as a base), a Pd(0)/PVP colloid exhibited slightly lower catalytic activity.

Keywords: Suzuki–Miyaura reaction; Nanostructured alumina–zirconia; Palladium nanoparticles; Metal colloid; Supported palladium

1. Introduction

Palladium-catalyzed C–C bond formation reactions are versatile tools in advanced organic synthesis [1–6]. Among these processes, a special place is occupied by the Suzuki–Miyaura reaction, an efficient method for preparing unsymmetrical biaryls from an aryl halide and boronic acid with a high tolerance to the presence of functional groups as the substituents [7,8]. The biaryls are important substrates in the synthesis of pharmaceuticals and herbicides [3].

Different palladium catalysts applied in the Suzuki–Miyaura reaction have been described in recent review articles [9–11]. Besides palladacycles [12] and *N*-heterocyclic carbene complexes [13–16], palladium nanoparticles also have been considered as catalytically active in phosphorus-free systems [17–20]. In most cases, Pd/PVP [21,22] or Pd/C [23] systems are used; however, there also are some examples of application of oxides as the supports for nanoparticles [24–27]. Solid supports, such as MgO [24], KF/Al_2O_3 [25], Al_2O_3 [26], MgLa [27], and LDH (double-layered hydroxide) [28], also have been used for palladium nanoparticle immobilization. The Suzuki–Miyaura reaction has been carried out mainly at rather elevated temperatures (80–120 °C) [9,29] or at long reaction times (>24 h) [30]. Little work has been published on efficient low-temperature heterogeneous Suzuki couplings [23,31].

When searching for a simple phosphorus-free catalytic system for the Suzuki–Miyaura reaction, we selected supports composed of binary oxides of the Al_2O_3–ZrO_2 type and characterized by good thermal and mechanic stability [32,33]. We modified their phase composition and the degree of surface hydroxylation by hydrothermal treatment to obtain the optimal support for Pd(0) nanoparticles. In addition, we prepared the Al_2O_3–ZrO_2 oxide containing 1% of Eu_2O_3 and tested it as a catalyst support. We expected to find that under the reaction conditions, Eu^{3+} could be reduced to Eu^{2+}, having strong re-

* Corresponding author.
E-mail address: ania@wchuwr.chem.uni.wroc.pl (A.M. Trzeciak).

0021-9517/$ – see front matter
doi:10.1016/j.jcat.2007.12.004

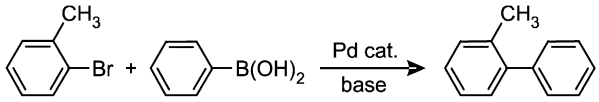

Scheme 1. Suzuki coupling of 2-bromotoluene with phenylboronic acid.

ducing properties and consequently facilitating stabilization of the catalytically active Pd(0) nanoparticles [34,35].

In this work, we obtained heterogenized palladium catalysts through impregnation of alumina-based oxides Al_2O_3, Al_2O_3–ZrO_2, and Al_2O_3–ZrO_2–Eu_2O_3 by an aqueous $PdCl_2$ solution. After the impregnation, palladium was reduced with methanol or hydrazine, and the catalysts thus obtained were tested in the Suzuki reaction (Scheme 1) carried out at 40, 60, and 80 °C. We also performed the Suzuki–Miyaura reactions with nonreduced supported $PdCl_2$ and with Pd/PVP or Pd/PVPy (PVP = polyvinylpyrrolidone, PVPy = polyvinylpyridine).

2. Experimental

2.1. Chemical reagents and substrates

Analytical-grade methanol, 2-propanol, *n*-hexane, *n*-dodecane, potassium hydroxide, nitric acid, and hydrochloric acid were purchased from POCh (Gliwice, Poland). Aluminum isopropoxide, zirconyl nitrate hydrate, europium nitrate, palladium dichloride, 2-bromotoluene, and poly(4-vinylpyridine) were acquired from Aldrich. Hydrazine hydrate (80%) was purchased from Riedel–de Haën. Phenylboronic acid and polyvinylpyrrolidone were supplied by Fluka. All of these chemical compounds were used as received with no further purification.

2.2. Synthesis of alumina–zirconia supports

The nanostructured Al_2O_3–ZrO_2 matrix containing 10% of zirconia was prepared in the following manner. First, 102 g of solid aluminum isopropoxide was hydrolyzed for 15 min in 600 cm^3 of distilled water at 90 °C with continuous stirring. The aluminum hydroxide, AlOOH, thus obtained was then peptized by slow addition of an aqueous solution of zirconyl nitrate hydrate (6.32 g in 50 cm^3 of water) also containing 2.86 cm^3 of 65% HNO_3 (zirconium to nitrate ions ratio 1:4). The resulting homogeneous mixture was refluxed at 90 °C for 72 h under stirring. The sol was condensed by evaporation and resulting gel was extruded in a wire form (2 mm in diameter) and dried. The wires were calcined at 500 °C for 4 h, and then divided into two parts, A and B. Part A was directly used as the catalyst support (sample A); part B was hydrothermally treated. In this treatment, 50 cm^3 of distilled water was placed on the bottom of a 1000-cm^3 stainless steel autoclave, and a glass vessel containing the support was introduced. The sample was not in a direct contact with the liquid water, but only with steam in the vapor phase. The autoclave was sealed and kept at 200 °C for 6 h. Then the autoclave was cooled and the support thus obtained was dried. One part of this support (sample B) was used directly for further experiments, whereas the other (sample C) was also calcined at 500 °C for 4 h. The alumina–zirconia with addition of Eu_2O_3 was prepared by impregnation of the Al_2O_3–ZrO_2 sample A in an aqueous solution of $Eu(NO_3)_3$ for 24 h. Then the sample was dried and calcined again at 500 °C for 4 h. The mixed oxide Al_2O_3–ZrO_2–Eu_2O_3 thus obtained, containing 1% of Eu_2O_3, was then used as the catalyst support (sample D).

2.3. Catalyst preparation procedures

2.3.1. Palladium supported on alumina-based oxides (methanol as reducing agent)

First, 0.8 g of the Al_2O_3–ZrO_2 support (sample A, B, C, or D) was impregnated in 10 cm^3 of an aqueous acidic solution ($C_{HCl} = 0.09$ mol/dm^3) of $PdCl_2$ containing 25 mg of Pd. After 72 h, the solution was decanted and the support was washed three times with water. Next, 50 cm^3 of methanol was added and refluxed for 45 min to reduce Pd(II) to Pd(0) nanoparticles. During heating, the sample changed in color from brown-orange to black. After refluxing, the catalyst thus obtained was dried in vacuo. The amount of the supported palladium was estimated by measuring the UV–vis absorption spectra of the solution that remained after the impregnation or by the ICP method.

2.3.2. Palladium supported on alumina-based oxides (hydrazine as reducing agent)

First, 0.8 g of the Al_2O_3–ZrO_2 support (sample A, B, C, or D) was impregnated in 10 cm^3 of an aqueous acidic solution ($C_{HCl} = 0.09$ mol/dm^3) of $PdCl_2$ containing 25 mg of Pd. After 72 h, the solution was decanted, and the support was washed three times with water. Next, 25 cm^3 of an aqueous solution containing 0.5 cm^3 of $N_2H_4{\cdot}H_2O$ (80%) was heated to 60 °C. Once the temperature was stabilized, the support containing Pd(II) was introduced to the hydrazine solution. Pd(II) was reduced to Pd(0) nanoparticles in 1 min, but the heating was continued for another 10 min. Finally, the catalyst thus obtained was dried in vacuo. The amount of the supported palladium was estimated by ICP of the solution remaining after the impregnation.

2.3.3. Preparation of Pd/PVP colloid—Pd(0) nanoparticles supported on PVP

One gram of PVP (average molecular weight, 40,000 or 10,000) was added to 20 cm^3 of water and intensively stirred until the polymer was totally dissolved. Next, 1 cm^3 of an aqueous solution containing 0.02 cm^3 of $N_2H_4{\cdot}H_2O$ (80%) was added. The solution was stirred for 20 min, then heated to 60 °C. Once the temperature was stabilized, 3.5 cm^3 of an acidic solution ($C_{HCl} = 0.18$ mol/dm^3) of $PdCl_2$ containing 17.5 mg of Pd was introduced, and the mixture was stirred intensively for 10 min. During stirring, the mixture changed in color to dark brown. The colloidal suspension thus obtained was dried completely in a rotary vacuum evaporator, yielding a film of PVP-stabilized Pd(0) colloid containing 1.75% of Pd.

2.3.4. Preparation of Pd(II) supported on PVPy

One gram of poly(4-vinylpyridine) (PVPy; average molecular weight, 160,000) or 2% cross-linked poly(4-vinylpyridine) (PVP 2% DVB) was added to 20 cm^3 of water and stirred intensively for 10 min. Then 3.5 cm^3 of an acidic solution ($C_{HCl} = 0.18$ mol/dm^3) of $PdCl_2$ containing 17.5 mg of Pd was introduced, and the mixture was stirred intensively for another 10 min. The polymer thus obtained, containing 1.75% of Pd(II), was filtered off and dried in vacuo.

2.3.5. Preparation of Pd(0) supported on PVPy

One gram of poly(4-vinylpyridine) (PVPy; average molecular weight, 160,000) or 2% cross-linked poly(4-vinylpyridine) (PVP 2% DVB) was added to 20 cm^3 of water and stirred intensively for 10 min. Then 1 cm^3 of an aqueous solution containing 0.02 cm^3 of $N_2H_4{\cdot}H_2O$ (80%) was added. The suspension was heated to 60 °C and stirred for another 10 min. Once the temperature was stabilized, 3.5 cm^3 of an acidic solution ($C_{HCl} = 0.18$ mol/dm^3) of $PdCl_2$ containing 17.5 mg of Pd was introduced, and the mixture was stirred intensively for another 10 min. The polymer thus obtained, containing 1.75% of Pd(0), was filtered off and dried in vacuo.

2.4. Suzuki–Miyaura catalytic test reactions

The catalytic tests were carried out in a 40-cm^3 Schlenk tube with magnetic stirring. The solid reagents, phenylboronic acid 0.135 g (1.1×10^{-3} mol) and potassium hydroxide 0.068 g (1.2×10^{-3} mol), were introduced first, followed by the liquids, 2-propanol or 2-propanol with water mixture (1:1) 10 cm^3 (used as a solvent), 2-bromotoluene 0.120 cm^3 (1.0×10^{-3} mol), and *n*-dodecane 0.100 cm^3 (the internal standard). Finally, supported catalyst (2.0×10^{-5} mol of Pd) was added. The reactor was sealed under nitrogen atmosphere and placed in a thermostatted oil bath. The catalytic reactions were carried out for 1 or 4 h. Once the reaction was complete, the reactor was cooled to ambient temperature and the organic components were extracted by intensive shaking for 5 min with two 5-cm^3 portions of *n*-hexane. After extraction, a small amount of water was added for the reactions carried out in 2-propanol, to facilitate separation of the liquid phases. A colorless *n*-hexane phase was transferred to a 10-cm^3 calibrated flask and analyzed by GC-MS (Hewlett–Packard 8452A). In most cases, the experiments were repeated 2 times and the results averaged (exact to 3%).

2.5. Support and catalyst characterization

The BET specific surface area, total pore volume, and pore size distribution of the Al_2O_3–ZrO_2 supports were determined from the corresponding N_2 adsorption–desorption isotherms (at the liquid nitrogen temperature) using a Fisons Sorptomatic 1900 automatic volumetric apparatus. Before the measurements, the samples were degassed at 250 °C and 10^{-3} Torr vacuum for 4 h. The pore size distribution was analyzed using the Dollimore–Heal method [36], assuming a cylindrical pore model.

The XRD measurements were carried out with a DRON-3 diffractometer operating with the Cu$K\alpha$ radiation line. The crystalline phases, γ-alumina, tetragonal zirconia, and monoclinic zirconia, were identified by referring to JCPDS card numbers 10-0425, 17-0923, and 37-1484, respectively. The average diameter of the supported palladium nanoparticles was estimated from the X-ray (111) line-broadening (measured at $2\theta = 40.1°$ with a step size of 0.01°) by means of the Debye–Scherrer equation.

The TEM measurements were carried out with a Philips CM-20 Super Twin microscope operating with an acceleration voltage of 200 kV and providing a resolution of 0.24 nm. The Pd(0) nanoparticle size distributions were determined by counting the size of approximately 50 particles on several TEM images obtained from different places on the TEM carbon grids. The size distribution plots were fitted by means of a Gauss curve approximation.

3. Results and discussion

3.1. Characteristics of alumina–zirconia supports

A TEM micrograph (Fig. 1) showing the sol precursor of the alumina–zirconia supports demonstrates the characteristic nanocrystalline structure of this material. The size distribution of the rod-shaped particles was fairly uniform, with an average width of about 5 nm and average length of about 30 nm. We also found that the nanostructure and the morphology of the material were preserved during the heat treatment at 500 °C. Furthermore, the TEM obtained for sample B exposed the morphology of zirconia nanocrystallites in the sample (Fig. 2). The ZrO_2 formed quasi-spherical particles, which may be easily recognized in the micrograph by characteristic lattice fringes, corresponding to atomic plane distances of 2.8, 3.0, and 3.2 Å. The diameter of the ZrO_2 particles was between 4 and 8 nm.

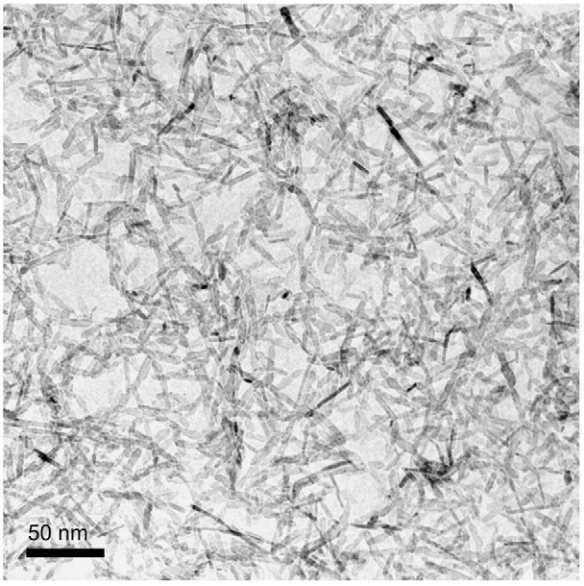

Fig. 1. TEM micrograph showing characteristic morphology of the obtained sol precursor (nanocrystalline pseudoboehmite in form of rod-shaped particles).

Table 1
Textural characteristics of the alumina-based supports and palladium loadings of the obtained catalysts

Sample	Support synthesis[a]	Specific surface area (m^2/g)	Total pore volume (cm^3/g)	Mean pore diameter (nm)	Pore size distribution		Catalyst Pd loading (wt%)[b]
					nm	%	
Al_2O_3	Sol–gel processing and calcination	210	0.28	2.5	2–10 0–2	79.1 20.9	1.5–1.8
Al_2O_3–ZrO_2 (A)	Sol–gel processing and calcination	218	0.27	2.2	2–10 0–2	75.6 24.4	1.6–1.9
Al_2O_3–ZrO_2 (B)	Sample A hydrothermally treated	202	0.24	2.0	2–10 0–2	52.8 47.2	1.4–1.7
Al_2O_3–ZrO_2 (C)	Sample B after additional calcination	208	0.30	2.8	2–10 0–2	85.5 14.5	1.4–1.7
Al_2O_3–ZrO_2–Eu_2O_3 (D)	Impregnation of sample A and calcination	182	0.25	2.7	2–10 0–2	81.8 18.2	1.9–2.2

[a] See Section 2 for detailed synthesis procedures.
[b] Minimum and maximum values determined by UV–vis (solution after impregnation) or ICP method for a few different samples.

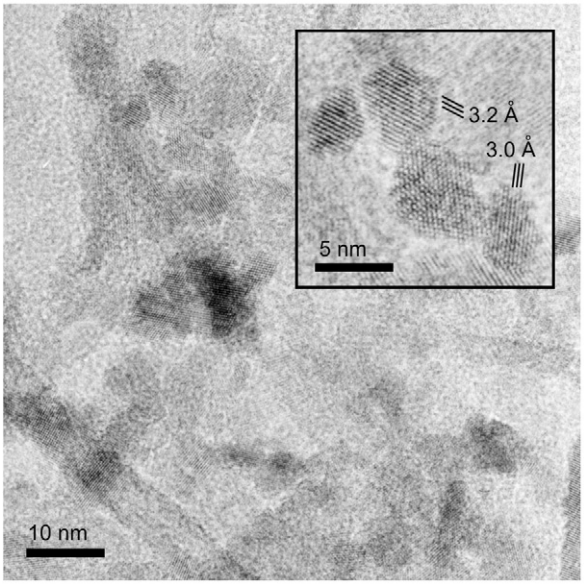

Fig. 2. Zirconia crystallites in the Al_2O_3–ZrO_2 (B) support. The tetragonal and monoclinic forms of ZrO_2 are both observed here (lattice fringes of 3.0 and 3.2 Å, respectively).

The XRD phase identification of the alumina–zirconia mixed oxides revealed characteristic signals at 37.6°, 45.8°, and 66.6°, which are attributed to the (311), (400), and (440) reflections of γ-Al_2O_3, respectively. No zirconia was detected for sample A, which might be explained by the fact that the samples contain very small ZrO_2 crystallites (below the XRD detection limit) or an amorphous ZrO_2 phase. It is known that only a limited amount of zirconia (<5%) can be incorporated into the structure of alumina to form a typical solid solution [37], and, consequently, the rest of the ZrO_2 must remain in the form of separate particles.

Besides the pattern characteristic for γ-Al_2O_3 phase, samples B and C showed diffraction peaks at 30.2°, 50.4°, and 59.8°, identified as (111), (202), and (311) reflections of tetragonal zirconia. In addition to the tetragonal ZrO_2 peaks, sample B also exhibited signals at 28.2°, 31.5°, and 49.2°. These peaks are recognized as reflections ($\bar{1}11$), (111), and (220), respectively, of the monoclinic phase. The volume fraction V_m of the monoclinic zirconia in sample B was about 75%, and the remaining part was present as the tetragonal form. This value was estimated by comparing the integral intensities of the tetragonal and the monoclinic reflections, using the equation proposed by Garvie [38] and Toraya [39]. In contrast, only the tetragonal form was observed for sample C (calcined once again at 500 °C after hydrothermal treatment).

The nitrogen adsorption–desorption studies revealed that the alumina–zirconia mixed oxides were highly porous (Table 1). The specific surface area and the pore volume were quite similar for all of the characterized samples, but the pore size distribution differed. Thus, samples C and D contained mostly larger pores (2–10 nm) with just a few smaller ones (0–2 nm), whereas sample B comprised almost equal numbers of small and large pores. Analysis of the isotherms leads to the identification of their profiles as type IV with H2 hysteresis loops, according to the IUPAC classification. This is typical for mesoporous materials and suggests that the pores might have uniform size and shape.

3.2. Palladium nanoparticles on alumina–zirconia

The palladium content on alumina-based oxides was practically the same for all of the catalysts obtained (Table 1); any slight differences could be linked to their varying textural properties. The highest palladium content was determined for the Al_2O_3–ZrO_2–Eu_2O_3 (D) support. The catalysts, in the form of immobilized Pd(0) nanoparticles, were characterized by XRD and TEM. A typical TEM image (Fig. 3) reveals palladium particles identified on a magnified high-resolution fragment by characteristic lattice fringes of 2.2 Å spacing, corresponding to the (111) planes of the FCC Pd(0) structure. The nanoparticles supported on alumina–zirconia were spherical, and none showed the typical crystal outlines frequently seen in palladium particles protected by polymers [40,41]. They were of similar size, demonstrated no aggregation, and were nearly uniformly dispersed on the surface of the support.

Table 2
Product yields obtained in the Suzuki–Miyaura reaction of 2-bromotoluene and phenylboronic acid (40 °C, 4 h)—influence of the reducing agent, solvent and reaction procedure

Catalyst	Reducing agent	Solvent	Yield of Suzuki coupling (%)[a]		
			Glass reactor (Fig. 4)	Schlenk tube	
$Pd(0)/Al_2O_3$	MeOH	$^{i}PrOH$	36–59[b]	46[c]	78
	Hydrazine	$^{i}PrOH + H_2O$	59–65[b]	62[c]	64
	MeOH	$^{i}PrOH + H_2O$	–		88
$Pd(0)/Al_2O_3–ZrO_2$ (A)	MeOH	$^{i}PrOH$	35–57[a]	45[c]	49 (90)[d]
	Hydrazine	$^{i}PrOH + H_2O$	50–63[b]	57[c]	72
	MeOH	$^{i}PrOH + H_2O$	–		97
$Pd(0)/Al_2O_3–ZrO_2$ (C)	MeOH	$^{i}PrOH$	9–29[b]	20[c]	69
	Hydrazine	$^{i}PrOH + H_2O$	1		50
	MeOH	$^{i}PrOH + H_2O$	–		89
$Pd(0)/Al_2O_3–ZrO_2–Eu_2O_3$ (D)	Hydrazine	$^{i}PrOH + H_2O$	26–45[b]	36[c]	65

[a] Reaction conditions: 2-bromotoluene 0.120 cm^3 (1.0×10^{-3} mol), phenylboronic acid 0.135 g (1.1×10^{-3} mol), KOH 0.068 g (1.2×10^{-3} mol), solvent 10 cm^3, catalyst (2.0×10^{-5} mol of Pd), 40 °C, 4 h.
[b] Minimum and maximum yield in four experiments.
[c] Average product yield obtained in four experiments.
[d] Powdered catalyst.

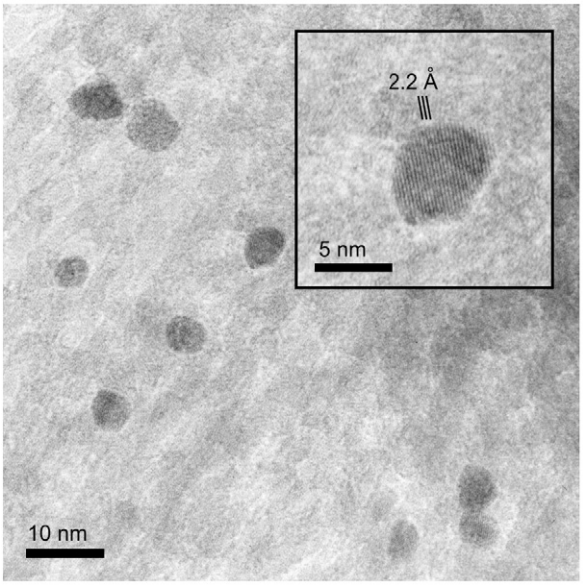

Fig. 3. Surface of the $Pd(0)/Al_2O_3–ZrO_2$ (A) catalyst (synthesized using methanol as the reducing agent) containing nearly uniformly dispersed palladium nanoparticles (characteristic lattice fringes of 2.2 Å).

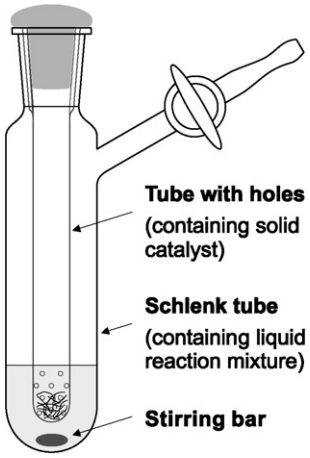

Fig. 4. Schematic view of the glass reactor enabling separation of the supported catalyst from the liquid reaction mixture—the solvent that is stirred flows through the tube containing the catalyst.

3.3. Suzuki–Miyaura coupling reaction

The Suzuki cross-coupling reactions were carried out in 2-propanol or 2-propanol with water mixture (1:1) at 40, 60, and 80 °C using KOH as the base. Such reaction conditions were chosen as optimal after a series of initial experiments in various solvents and with addition of different bases. A 2-propanol–water (1:1) mixture was found to be the best solvent; the positive affect of water can be explained by its ability to dissolve boron side products coating the catalyst surface.

It is noteworthy that for all of the alumina-supported catalysts, good or even very good results were obtained at temperatures as low as 40 °C. Early experiments carried out in a glass reactor consisting of a Schlenk tube with an additional internal container holding the supported catalyst (Fig. 4) gave poorly repeatable results, with as much as a 20% difference in product yields obtained under identical reaction conditions (Table 2). The low yields obtained in the glass reactor can be explained by the limited contact of reactants with the catalyst despite intensive stirring of the solution.

Much better repeatability and higher yields of the Suzuki–Miyaura reaction were obtained in experiments carried out in a standard Schlenk tube. Under such conditions, some amount of the supported catalyst underwent dispersion, which likely facilitated better contact of the substrates with active centers on the catalyst surface. Moreover, the product yield was greater when powdered catalyst was used in the Suzuki reaction (Table 2).

The results presented in Table 2 demonstrate two characteristic effects controlled by the catalyst preparation method used

Table 3
Yields of the Suzuki–Miyaura reaction of 2-bromotoluene and phenylboronic acid carried out at various temperatures and catalyzed by Pd(0) nanoparticles (prepared by reduction with hydrazine) supported on different solid supports (reaction time 4 h)

Catalyst	Yield of Suzuki coupling (%)[a]				Nanoparticles size (nm)[b]			
	40 °C	60 °C	80 °C[c]	80 °C	Before reaction	After reaction at temperature		
						40 °C	60 °C	80 °C
$Pd(0)/Al_2O_3$	64	98	84	96	11.7	11.4	11.8	11.6
$Pd(0)/Al_2O_3$–ZrO_2 (A)	72	95	96	99	12.1	11.8	12.1	12.1
$Pd(0)/Al_2O_3$–ZrO_2 (B)	91	99	99	98	11.3	10.6	11.2	11.9
$Pd(0)/Al_2O_3$–ZrO_2 (C)	50	95	71	96	11.3	11.5	11.0	11.2
$Pd(0)/Al_2O_3$–ZrO_2–Eu_2O_3 (D)	65	93	87	99	11.7	11.4	11.1	12.1

[a] Reaction conditions: 2-bromotoluene 0.120 cm^3 (1.0×10^{-3} mol), phenylboronic acid 0.135 g (1.1×10^{-3} mol), KOH 0.068 g (1.2×10^{-3} mol), $^iPrOH + H_2O$ 5 + 5 cm^3, catalyst (2.0×10^{-5} mol of Pd), 4 h.
[b] Estimated from the X-ray (111) line broadening measured at $2\theta = 40.1°$.
[c] Reaction time: 1 h.

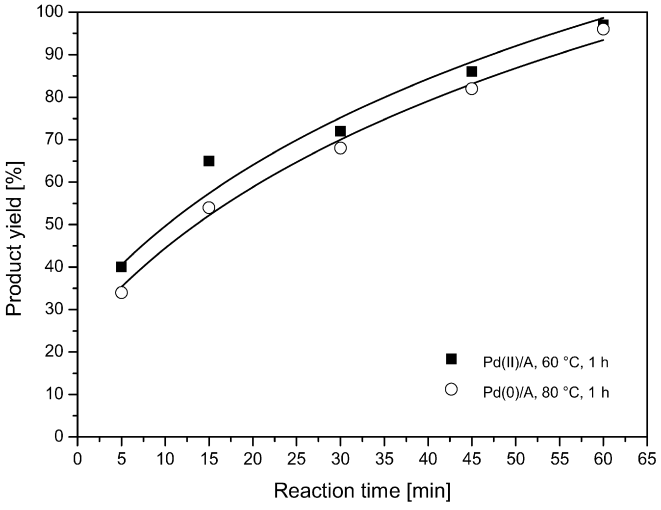

Fig. 5. Reaction kinetics of the Suzuki–Miyaura coupling of 2-bromotoluene with phenylboronic acid catalyzed by palladium supported on Al_2O_3–ZrO_2 (A).

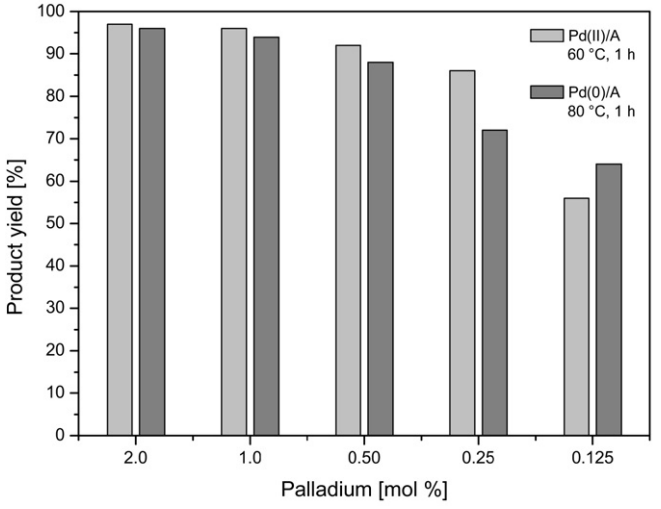

Fig. 6. Influence of the catalyst concentration on the yield of the Suzuki cross-coupling of 2-bromotoluene with phenylboronic acid catalyzed by palladium supported on Al_2O_3–ZrO_2 (A).

and the type of solvent applied. The average size of the Pd(0) nanoparticles obtained by reduction of Pd(II) with methanol was ca. 7 nm, whereas the particles formed by reduction with hydrazine were slightly larger (ca. 11 nm). Smaller palladium nanoparticles are more active; however, particle size may not be the only factor affecting catalytic activity in the Suzuki reaction.

The yield of 2-methylbiphenyl obtained in the Suzuki–Miyaura reaction increased with increasing temperature, reaching >90% after 4 h at 60 and 80 °C for all of the supported catalysts (Table 3). The kinetic studies carried out for the $Pd(0)/Al_2O_3$–ZrO_2 catalyst (sample A) at 80 °C demonstrated that the reaction starts without an induction period and that the yield gains 34% after just 5 min (Fig. 5). The product yield determined after 1 h decreased with decreasing catalyst concentration, from 96% for 1 mol% of palladium to 64% for 0.125 mol% of palladium (Fig. 6). There are very attractive results, especially for a heterogeneous catalyst. The main product, 2-methylbiphenyl, was formed with high selectivity, and only up to 3% of biphenyl (the homocoupling product) was found in some reactions. The XRD measurements performed after the Suzuki reaction lead us to conclude that Pd(0) nanoparticle size remained practically unchanged (about 11 nm) before and after the reaction, independent from temperature (Table 3). Similarly supported Pd(0) nanoparticles obtained by reduction with methanol (of ca. 5 nm in diameter) also remained unchanged during the Suzuki reaction (Fig. 8, see below).

The catalysts in the unreduced form—Pd(II) on alumina-based oxides—turned out to be even more active than those that were reduced before application. They produced between 88% and 100% of 2-methylbiphenyl after 4 h at 40 °C. Similar results were obtained at 60 °C after just 1 h (Table 4). XRD studies of these catalysts confirmed the presence of Pd(0) nanoparticles ranging in size from 6.6 to 8.2 nm. This demonstrates that the impregnated $PdCl_2$ underwent rapid reduction in situ under the Suzuki reaction conditions, and that such palladium nanoparticles used in statu nascendi were even more active than those prepared earlier by special reduction procedures. Reduction of Pd(II) by 2-propanol used as a solvent was quite fast and occurred almost immediately after introduction of the catalyst [Pd(II) supported on alumina-based oxide] to the reaction mixture.

In addition to the above-described experiments, the Suzuki–Miyaura reaction catalyzed by Pd(0) supported on PVP (PVP = polivinylpyrrolidone) of two different molecular weights (10,000 and 40,000) was carried out for comparison. The molecular weight of the polymer had a significant influence on the catalytic activity of such systems, which was higher when the polymer of lower molecular weight was used (Table 5). The observed differences in reactivity are most likely related to the polymer structure, because they cannot be explained solely by the different average sizes of the Pd(0) nanoparticles (5.5 vs 7.3 nm). It is noteworthy that the better catalyst, Pd(0)/PVP-10,000, was only slightly less active (84%) than the alumina-supported systems (96%) (Table 6).

To continue the studies on the polymer influence on the catalytic activity, we performed several additional experiments. Polyvinylpyridines (polyvinylpyridine, PVPy and polyvinylpyridine cross-linked with 2% of divinylbenzene, PVPy 2% DVB) were used as the supports for Pd(II) and Pd(0) nanoparticles. Both the supported catalysts containing Pd(0) appeared to be weak and produced only 5 and 8% of product, respectively at 80 °C after 1 h (Table 6). Slightly better results, 12 and 20%, were obtained for the Pd(II) precursors. In addition, polyvinylpyridine was identified as a very strong inhibitor of the reaction catalyzed by Pd(0)/Al_2O_3–ZrO_2 (A) and Pd(II)/Al_2O_3–ZrO_2 (A), causing a decrease in the yield from 96–97% to only 2–8%. Similar results were considered to provide evidence of solubilization of palladium during the reaction [42]. In contrast to the literature data [43], we found that pyridine also acted as an inhibitor of the Suzuki–Miyaura reaction catalyzed by Pd(0)/Al_2O_3–ZrO_2 (A) (Table 6). Similarly, PVP polymers caused a decrease in the reaction yields; the influence of PVP-40000 was particularly significant. In the presence of this polymer, the yield dropped to 32% with Pd(0)/Al_2O_3–ZrO_2 (A) and to 22% with Pd(II)/Al_2O_3–ZrO_2 (A). Thus, the product yields were much lower than obtained when Pd(0)/PVP-40000 was used as a catalyst. An inhibiting effect of PVP also was observed in the Suzuki–Miyaura reaction catalyzed by Pd/PVP [22].

Table 4
Results of the Suzuki–Miyaura cross-coupling reaction catalyzed by $PdCl_2$ supported on different alumina-based oxides

Catalyst (initial form)	Yield of Suzuki coupling (%)[a]		Nanoparticles size after reaction (nm)[b]
	40 °C, 4 h	60 °C, 1 h	40 °C, 4 h
Pd(II)/Al_2O_3	88	82	8.2
Pd(II)/Al_2O_3–ZrO_2 (A)	95	97	7.2
Pd(II)/Al_2O_3–ZrO_2 (B)	100	99	6.6
Pd(II)/Al_2O_3–ZrO_2 (C)	98	81	7.1
Pd(II)/Al_2O_3–ZrO_2–Eu_2O_3 (D)	99	84	7.7

[a] Reaction conditions: 2-bromotoluene 0.120 cm^3 (1.0×10^{-3} mol), phenylboronic acid 0.135 g (1.1×10^{-3} mol), KOH 0.068 g (1.2×10^{-3} mol), ^{i}PrOH + H_2O 5 + 5 cm^3, catalyst (2.0×10^{-5} mol of Pd(II)).
[b] Estimated from the X-ray (111) line broadening measured at $2\theta = 40.1°$.

3.4. Palladium catalysts before and after the Suzuki reaction

It is possible to conclude from some of the TEM micrographs (Fig. 7) that the palladium particles are typically located in the pores of the alumina–zirconia support and are only sterically constrained there. As a result, they probably are not strongly attached to the alumina-based solid support.

Table 5
Comparison of the yields of the Suzuki–Miyaura coupling at various temperatures catalyzed by Pd(0)/PVP colloids (reaction time 4 h)

Catalyst (nanoparticles size)	Suzuki reaction yield (%)[a]				
	40 °C		60 °C		80 °C
	^{i}PrOH	^{i}PrOH + H_2O	^{i}PrOH	^{i}PrOH + H_2O	^{i}PrOH + H_2O
Pd(0)/PVP-40000 (7.3 nm)	3	27	26	60	75
Pd(0)/PVP-10000 (5.5 nm)	55	74	77	87	90

[a] Reaction conditions: 2-bromotoluene 0.120 cm^3 (1.0×10^{-3} mol), phenylboronic acid 0.135 g (1.1×10^{-3} mol), KOH 0.068 g (1.2×10^{-3} mol), ^{i}PrOH + H_2O 5 + 5 cm^3, catalyst (2.0×10^{-5} mol of Pd).

Table 6
Influence of the additives on the catalytic activity of Pd(0) nanoparticles (obtained by reduction with hydrazine) immobilized on Al_2O_3–ZrO_2 (A) and the results of the Suzuki–Miyaura reaction catalyzed by palladium supported on poly(4-vinylpyridine) or polyvinylpyrrolidone

Catalyst	Catalytic reaction conditions	Product yield (%)[a]						
		No additives	Additives					
			PVP-10000	PVP-40000	PVPy	PVPy added after 5 min	PVPy 2% DVB	Pyridine
Pd(0)/Al_2O_3–ZrO_2 (A)	80 °C, 1 h	96	84	32	2	37	5	78
Pd(II)/Al_2O_3–ZrO_2 (A)	60 °C, 1 h	97	76	22	6	41	8	48
Pd(0)/PVPy	80 °C, 1 h	5	–	–	–	–	–	–
Pd(0)/PVPy (2% DVB)	80 °C, 1 h	8	–	–	–	–	–	–
Pd(II)/PVPy	80 °C, 1 h	12	–	–	–	–	–	–
Pd(II)/PVPy (2% DVB)	80 °C, 1 h	20	–	–	–	–	–	–
Pd(0)/PVP-40000	80 °C, 1 h	45	–	–	–	–	–	–
Pd(0)/PVP-10000	80 °C, 1 h	74	–	–	–	–	–	–

[a] Reaction conditions: 2-bromotoluene 0.120 cm^3 (1.0×10^{-3} mol), phenylboronic acid 0.135 g (1.1×10^{-3} mol), KOH 0.068 g (1.2×10^{-3} mol), ^{i}PrOH + H_2O 5 + 5 cm^3, catalyst (2.0×10^{-5} mol of Pd).

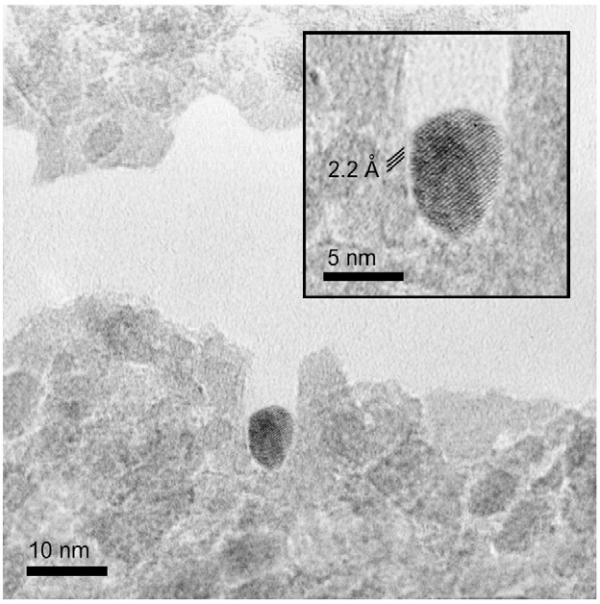

Fig. 7. High-resolution TEM micrograph revealing a single Pd(0) nanoparticle (reducing agent—methanol) anchored in a pore of mixed-oxide support Al_2O_3–ZrO_2 (C).

At this point, it is important to call attention to the results presented in Table 3, which show that the size of Pd(0) nanoparticles was not significantly affected during the Suzuki reaction. Further studies with application of the XRD and TEM measurements confirmed this observation (Table 7). Particularly essen-

Table 7
XRD and TEM determined Pd(0) nanoparticles size before and after the Suzuki coupling reaction (catalysts synthesized with use of methanol as the reducing agent)

Catalyst	Nanoparticles size (nm) determined from	
	XRD[a]	TEM[b]
Pd(0)/Al_2O_3–ZrO_2 (A)		
Fresh catalyst	7.1	5.6 ± 1.4
After reaction	7.0	5.3 ± 1.7
Pd(0)/Al_2O_3–ZrO_2 (B)		
Fresh catalyst	9.2	–
After reaction	8.4	–
Pd(0)/Al_2O_3–ZrO_2 (C)		
Fresh catalyst	6.8	5.3 ± 1.6
After reaction	6.7	5.2 ± 1.9

[a] Estimated from the X-ray (111) line broadening measured at $2\theta = 40.1°$.
[b] Center and FWHM of the Gauss curve fit of nanoparticles size distribution.

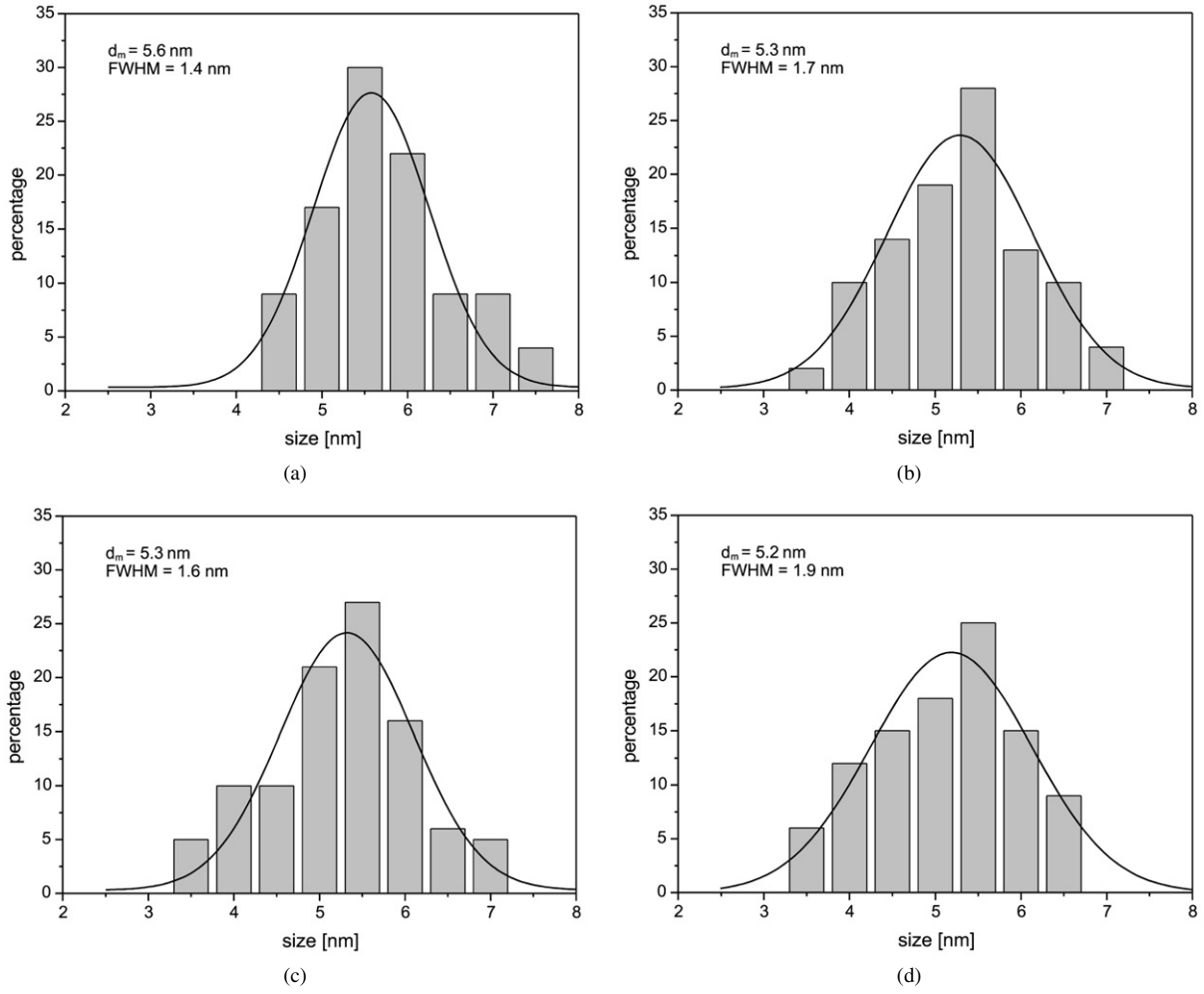

Fig. 8. Nanoparticle size distributions in the following systems (catalysts obtained by reduction with methanol): Pd(0)/Al_2O_3–ZrO_2 (A) catalyst as-prepared (a) and recovered after one reaction run (b), Pd(0)/Al_2O_3–ZrO_2 (C) catalyst as-prepared (c) and recovered after one reaction run (d).

tial is the conclusion resulting from the TEM studies; not only did the average nanoparticle size remain practically unchanged, but also the size distribution remained essentially the same during the reaction (Fig. 8). Other authors have reached a similar conclusion [22]. This contradicts the results from our previous studies of PVP-protected Pd(0) colloids in the Heck reaction of bromobenzene and butyl acrylate [44] or methoxycarbonylation of iodobenzene [45], which found dramatic changes in particle size distribution. Redispersion of Pd(0) particles supported on nanostructured alumina pellets also was observed in the Heck reaction carried out in molten [^{n}Bu$_4$N]Br salt [46]. All Pd(0) nanoparticles studied in the present work were spherical, with no well-defined geometrical shapes. According to our previous results [45], typical crystal forms (with many edges) would be expected to be even more active.

4. Conclusion

Alumina-based oxides Al_2O_3, Al_2O_3–ZrO_2 (A, B, C), and Al_2O_3–ZrO_2-Eu_2O_3 (D) have been synthesized and used as the supports for immobilization of catalytically active palladium nanoparticles. Depending on the preparation procedure, these materials are characterized by various textural properties and slightly different structures. Especially worth emphasizing is the fact that the obtained nanoparticulate catalysts revealed their high potential in the Suzuki–Miyaura cross-coupling reaction, especially when compared with conventional phosphorous-free catalytic systems, such as Pd/C or Pd(0) nanoparticles protected by polymers. The test reaction proceeded efficiently under very mild conditions at temperature as low as 40 °C, and the activity increased significantly at 60 and 80 °C. This important finding, together with all of the advantageous mechanical properties (i.e., high thermal stability, very good wear resistance, and rather uncomplicated separation from the reaction mixture by simple filtration), makes these catalysts excellent candidates for practical applications.

Very high reaction yields also were noted when $PdCl_2$ supported on mixed oxides was used without earlier palladium(II) reduction. These catalysts were even more active than those that had been reduced before application, producing almost 100% of 2-methylbiphenyl after just 1 h at 60 °C. XRD confirmed that Pd(0) nanoparticles were formed here in situ during the catalytic process.

Finally, some mechanistic studies of the presented systems showed that the size of palladium nanoparticles did not change during the Suzuki reaction. Their redispersion was hardly noticeable in this case. Consequently, it might be postulated that Suzuki–Miyaura coupling proceeds mainly on the surface of the particles. However, the detailed investigation of catalyst leaching, either in form of palladium complexes or unsupported Pd(0) nanoparticles, was not addressed in this work.

Acknowledgments

This research was supported by the Polish Ministry of Science and Higher Education through project PBZ-KBN-116/T09/2004. The financial support is gratefully acknowledged.

References

[1] B. Cornils, W.A. Herrmann (Eds.), Applied Homogeneous Catalysis with Organometallic Compounds, A Comprehensive Handbook, vols. 1, 2, VCH, Weinheim, 1996.
[2] F. Diederich, P.J. Stang (Eds.), Metal-Catalyzed Cross-Coupling Reactions, VCH, Weinheim, 1997.
[3] M. Beller (Ed.), Transition Metals for Organic Synthesis; Building Blocks and Fine Chemicals, VCH, Weinheim, 2004.
[4] I.P. Beletskaya, A.V. Cheprakov, Chem. Rev. 100 (2000) 3009.
[5] A.M. Trzeciak, J.J. Ziółkowski, Coord. Chem. Rev. 249 (2005) 2308.
[6] A.M. Trzeciak, J.J. Ziółkowski, Coord. Chem. Rev. 251 (2007) 1281.
[7] N. Miyaura, T. Yanagi, A. Suzuki, Synth. Commun. 11 (1981) 513.
[8] N. Miyaura, A. Suzuki, Chem. Rev. 95 (1995) 2457.
[9] F. Bellina, A. Carpita, R. Rossi, Synthesis (2004) 2419.
[10] R.B. Bedford, C.S.J. Cazin, D. Holder, Coord. Chem. Rev. 248 (2004) 2283.
[11] N.T.S. Phan, M. Van Der Sluys, C.W. Jones, Adv. Synth. Catal. 348 (2006) 609.
[12] M. Beller, H. Fischer, W.A. Herrmann, K. Ofele, C. Brossner, Angew. Chem. Int. Ed. Engl. 34 (1995) 1848.
[13] M.B. Andrus, C. Song, Org. Lett. 3 (23) (2001) 3761.
[14] E.A.B. Katchev, C.J. O'Brien, M.G. Organ, Aldrichim. Acta 39 (2006).
[15] O. Navarro, R.A. Kelly III, S.P. Nolan, J. Am. Chem. Soc. 125 (2003) 16194.
[16] F. McLachlan, C.J. Mathews, P.J. Smith, T. Welton, Organometallics 22 (2003) 5350.
[17] M.T. Reetz, E. Westermann, Angew. Chem. Int. Ed. 39 (1) (2000) 165.
[18] J.G. De Vries, Dalton Trans. (2006) 421.
[19] D. Astruc, Inorg. Chem. 46 (2007) 1884.
[20] J. Hu, Y. Liu, Langmuir 21 (2005) 2121.
[21] R. Narayanan, M.A. El-Sayed, J. Catal. 234 (2005) 348.
[22] R. Narayanan, M.A. El-Sayed, J. Am. Chem. Soc. 125 (2003) 8340.
[23] F.-X. Felpin, T. Ayad, S. Mitra, Eur. J. Org. Chem. (2006) 2679.
[24] M.L. Kantam, S. Roy, M. Roy, B. Sreedhar, B.M. Choudary, Adv. Synth. Catal. 347 (15) (2005) 2002.
[25] G.W. Kabalka, R.M. Pagui, C.M. Hair, Org. Lett. 1 (9) (1999) 1423.
[26] D. Kudo, Y. Masui, M. Onaka, Chem. Lett. 36 (7) (2007) 918.
[27] A. Cwik, Z. Hell, F. Figueras, Org. Biol. Chem. 3 (24) (2005) 4307.
[28] B.M. Choudary, S. Mahdi, N.S. Chowdari, M.L. Kantam, B. Sreedhar, J. Am. Chem. Soc. 124 (2002) 14127.
[29] A. Suzuki, J. Organomet. Chem. 576 (1999) 147.
[30] A. Desforges, R. Backov, H. Deluze, O. Mondain-Montval, Adv. Funct. Mater. 15 (2005) 1689.
[31] H. Sajiki, T. Kurita, A. Kozaki, G. Zhang, Y. Kitamura, T. Maegawa, K. Hirota, Synthesis (2005) 537.
[32] S. Castillo, M. Morán-Pineda, R. Gómez, Catal. Commun. 2 (2001) 295.
[33] J. Wrzyszcz, M. Zawadzki, A.M. Trzeciak, W. Tylus, J.J. Ziółkowski, Catal. Lett. 93 (2004) 85.
[34] R. Leboda, V.A. Tertykh, V.V. Sidorchuk, J. Skubiszewska-Zięba, Colloids Surf. A Physicochem. Eng. Aspects 135 (1998) 253.
[35] D. Enache, M. Roy-Auberger, K. Esterle, R. Revel, Colloids Surf. A Physicochem. Eng. Aspects 220 (2003) 223.
[36] D. Dollimore, G.R. Heal, J. Appl. Chem. 14 (1964) 109.
[37] I.M. Low, R. McPherson, J. Mater. Sci. 24 (1989) 892.
[38] R.C. Garvie, P.S. Nicholson, J. Am. Ceram. Soc. 56 (1972) 303.
[39] H. Toraya, M. Yoshimura, S. Somiya, J. Am. Ceram. Soc. 67 (1984) 119.
[40] H.P. Choo, K.Y. Liew, W.A.K. Mahmood, H. Liu, J. Mater. Chem. 11 (2001) 2906.
[41] H.P. Choo, K.Y. Liew, H. Liu, J. Mater. Chem. 12 (2002) 934.
[42] M. Weck, C.W. Jones, Inorg. Chem. 46 (2007) 1865.

[43] S. Klingelhöfer, W. Heitz, A. Greier, S. Oestreich, S. Förster, M. Antonietti, J. Am. Chem. Soc. 119 (1997) 10116.
[44] A. Gniewek, A.M. Trzeciak, J.J. Ziółkowski, L. Kępiński, J. Wrzyszcz, W. Tylus, J. Catal. 229 (2005) 332.
[45] A. Gniewek, J.J. Ziółkowski, A.M. Trzeciak, L. Kępiński, J. Catal. 239 (2006) 272.
[46] I. Pryjomska-Ray, A. Gniewek, A.M. Trzeciak, J.J. Ziółkowski, W. Tylus, Top. Catal. 40 (1–2) (2006) 173.